Zeszyty Naukowe Politechniki Częstochowskiej
Budownictwo – Civil Engineering Science
ISSN 0526-5916

Zeszyty Naukowe Politechniki Częstochowskiej nr 29 (2023), 79-84
DOI: 10.17512/znb.2023.1.12

An experimental and numerical evaluation of the mechanical properties of 3D prints made by Fused Filament Fabrication

Piotr Lacki[1], Anna Derlatka[2], Marcin Kwapisz[3], Aneta Idziak-Jabłońska[4]

ABSTRACT:
The paper presents the results of experimental research as well as numerical calculations of 3D printouts made using Fused Filament Fabrication (FFF) made of PLA filament. The aim of the work was to determine the mechanical properties of the printouts. It was observed that the modulus of elasticity of the printouts does not depend on the geometry of the samples nor the direction of the printouts. Conversely, the tensile strength and strains of the prints do depend on the geometry and the direction of the prints in relation to the direction of loading.

KEYWORDS:
print 3D; FFF; tensile test; FEM

1. Introduction

In recent years, rapid development of 3D printing has been observed. To a large extent, this is related to the increased access to devices as prices decrease. 3D printing is an example of an innovative approach to the issues of manufacturing technology. Currently, 3D printing is being used in every field related to design and manufacturing. Initially, it was only applied to the construction of prototypes. The development of modern technologies has enabled not only the creation of innovative prototypes, but also spare parts with special properties. Entire devices with small dimensions are often made. Easy access to devices enabling 3D printing and consumables means that unit production is also based on this technology [1-3]. Implementation of 3D printing, despite the large variety of solutions, boils down to the basic principle of applying successive layers of construction material. Current 3D printing techniques can be divided into four types: FDM/FFF (Fused Deposition Modeling/Fused Filament Fabrication), SLA (Stereolithography), SLS (Selective Laser Sintering) and CJP (Color Jet Printing).

The FDM/FFF printing method comes from the acronyms Fused Deposition Modeling and Fused Filament Fabrication, which means printing from molten plastic. This method is the most common due to the relatively simple technical solution and low cost of printing. It consists of laying layers of filament extruded through the nozzle, which is heated to a predetermined melting point depending on the parameters of the filament material. The software controls the movement direction of the head and the speed of filament extrusion. The next layer is applied by raising

[1] Czestochowa University of Technology, Faculty of Civil Engineering, ul. Akademicka 3, 42-218 Częstochowa, Poland, e-mail: piotr.lacki@pcz.pl, orcid id: 0000-0002-0787-8890
[2] Czestochowa University of Technology, Faculty of Civil Engineering, ul. Akademicka 3, 42-218 Częstochowa, Poland, e-mail: anna.derlatka@pcz.pl, orcid id: 0000-0002-6509-2706
[3] Czestochowa University of Technology, Faculty of Production Engineering and Materials Technology, al. Armii Krajowej 19, 42-201 Czestochowa, e-mail: marcin.kwapisz@pcz.pl, orcid id: 0000-0002-8534-1706
[4] Czestochowa University of Technology, Faculty of Mechanical Engineering and Computer Science, al. Armii Krajowej 21, 42-201 Czestochowa, e-mail: a.idziak-jablonska@pcz.pl, orcid id: 0000-0002-9859-1982

the printing nozzle by the thickness of the previous layer or lowering the working table. This depends on the construction of the 3D printer [1, 2, 4, 5].

The accuracy of the prints depends on the diameter of the nozzle, the precision of its positioning system, but above all on the solidification properties of the filament. Due to the layering methodology, printing is mostly done with one type of filament. In the newest devices, solutions with several heads are implemented, allowing for two-colour printouts. However, due to the cost of the device, they are not widely used. Another disadvantage of the FFF method is the need to place the printed layer on a backing. In addition, support is necessary for the dissolved filament before it solidifies. Therefore, it is not possible to print elements protruding from the surface of the object without additional printing of special supports [4, 5]. When printing with the FDM/FFF method, two materials are most often used: ABS (Acrylonitrile Butadiene Styrene) and PLA (polylactide, otherwise polylactic acid) [4]. The choice of material depends on the printed element and the properties which it should have.

2. Goal and scope of work

The aim of the work was to determine the mechanical properties of 3D prints made using Fused Filament Fabrication (FFF) made of PLA filament. The scope of the work included experimental research as well as numerical calculations.

2.1. Methodology of experiment

As part of the experimental tests, a static tensile test of the printouts with shapes in accordance with the ISO-3167 Plastics – Multipurpose test specimens standard [6] (Fig. 1a) and the ASTM D638-14 Standard Test Method for Tensile Properties of Plastics standard [7] (Fig. 1b) was carried out.

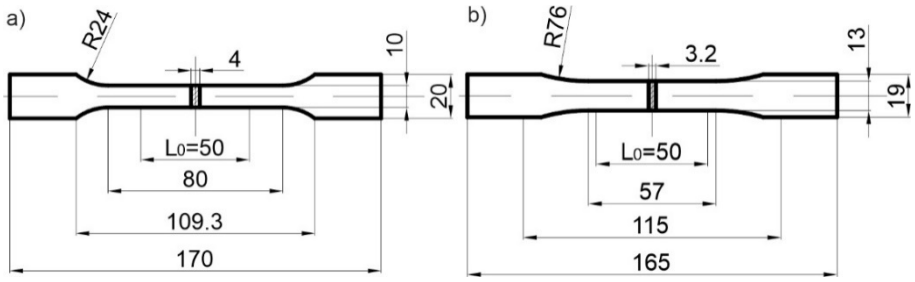

Fig. 1. Sample shape in accordance with the standard: a) ISO-3167 Plastics – multipurpose test specimens [6], b) ASTM D638-14 Standard Test Method for Tensile Properties of Plastics [7]

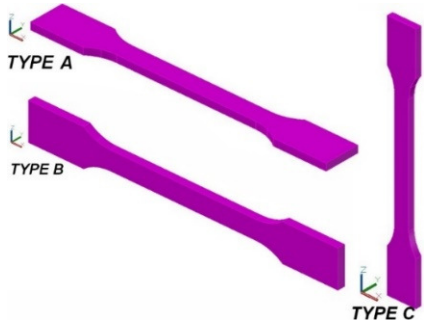

Fig. 2. Sample types that differ in the direction of printing along the Z axis, along which the increment occurred

For each of two shapes, three types of samples were printed, differing in the position of the printouts relative to the axis along which the increment took place (Z axis), as shown in Figure 2. As a result, 6 series of samples were obtained. In order to verify the repeatability of the results, 10 samples were made in each series.

The static tensile test was carried out using the ARAMIS optical deformation analysis system, thanks to which distributions of total strains were obtained.

2.2. Numerical calculations

The experimentally obtained strain-stress curves were used to develop numerical models. The numerical models were validated with the results from the experimental studies.

The numerical analysis was carried out using ADINA v. 9.8 software based on the finite element method. In this stages of the work, geometrical, discrete and numerical models of the samples were developed. A multilinear elastic-plastic model of the material was also produced.

A finite element mesh was generated for the performed geometric models. The discretization was carried out using 8-node 3D-SOLID finite elements. The total number of 3D elements equalled 4472 for the samples according to the ISO standard and 5720 for the samples according to the ASTM standard. Figure 3 shows a sample model with a finite element mesh and boundary conditions taken into account.

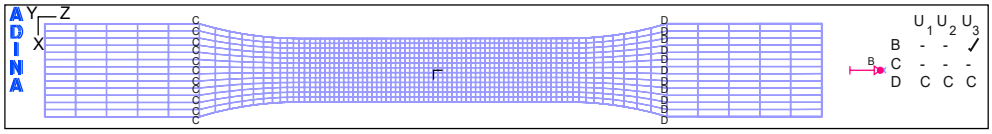

Fig. 3. Mesh of FEM model with marked boundary conditions

3. Results

The experimental tests and numerical calculations made it possible to obtain stress-strain diagrams and distributions of plastic strains on the surface of the analysed samples.

3.1. Experimental tests

The engineering stress-engineering strain diagrams for selected samples are shown in Figure 4. The distribution of strains before and after fracture is shown in Figures 5 and 6. One sample with geometry in accordance with ISO-3167 and ASTM D638 and for each A, B, C was selected.

It was observed that in the case of the type A samples with geometry based on the ISO and ASTM standards and for type B samples according to the ASTM standard, the strain – stress curve in the initial phase assumes a rectilinear character. This is followed by a short curvilinear section before the maximum tensile stress is reached. After exceeding the tensile strength R_m, a significant increase in strains with a slight decrease in stress until destruction occurred. Such a curve proves the elastic-plastic model of behaviour.

This was also confirmed by the strain distributions shown in Figures 5 and 6. In the case of the type A samples based on the ISO and ASTM and for the type B sample based on ASTM, strains were observed both during the affecting of tensile force and after the destruction of the samples.

However, in the case of type B and C samples based on the ISO standard and for the type C sample based on ASTM, the strain – stress curves become rectilinear and then the damage occurred. As a result, only the elastic nature of the behaviour of the prints can be specified.

This is also confirmed by the strains distributions shown in Figures 5b, c and 6c, where strains were observed only during the application of the tensile force. After failure, the strains are close to 0.0, i.e. the samples returned to their original geometry after the load was released.

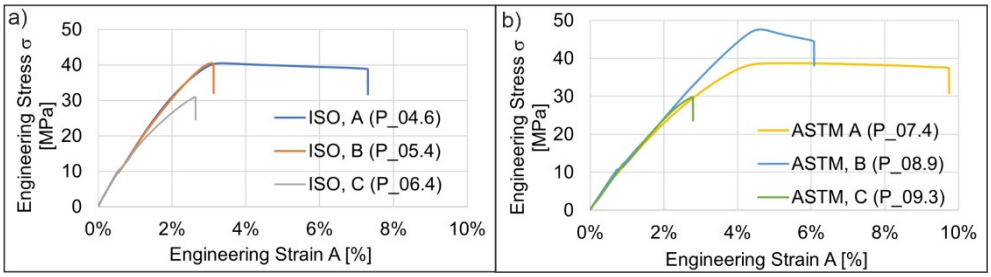

Fig. 4. Engineering strains – engineering stress diagrams for samples with geometry according to the following standards: a) ISO-3167, b) ASTM D638

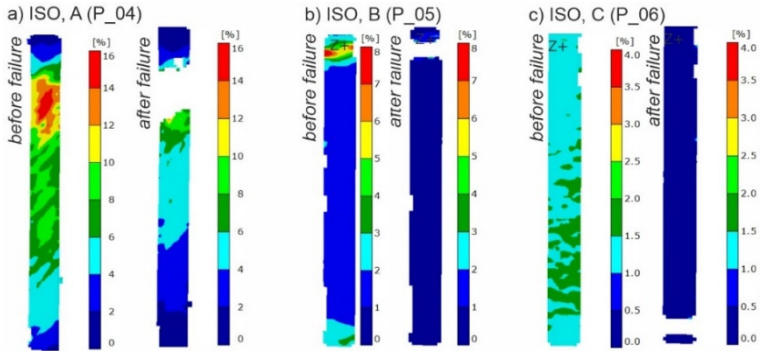

Fig. 5. Distributions of strains on samples with geometry in accordance with ISO-3167

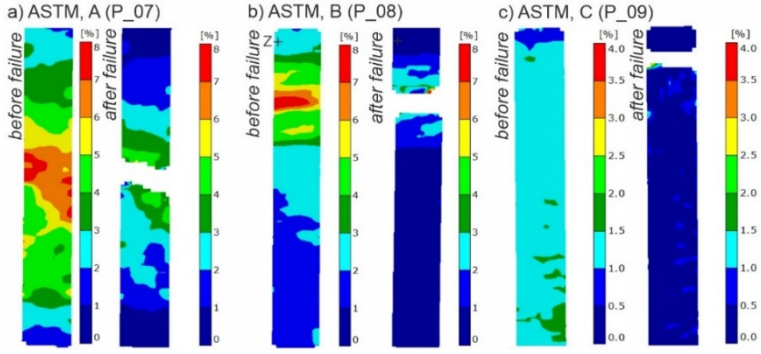

Fig. 6. Distributions of strains on samples with geometry in accordance with ASTM D638

Based on Figure 4, it was observed that in the case of prints with identical geometry, regardless of the print type, the strain-stress curves coincide in the initial loading phase, where the curves assume a rectilinear character. It proves that the modulus of elasticity of the printouts is not dependent on the direction of the printout.

3.2. Numerical calculations

For the prepared models, the state of effective stresses and strains was determined, shown in Figure 7. The range of effective stress values was from 0 to 46.8 MPa. The minimum stress values occur at the ends of the sample, in the place of the handles. The extreme is located in the measuring part, i.e. in the area of the smallest cross-sectional area. The values of plastic deformations in the measuring part are 0.015.

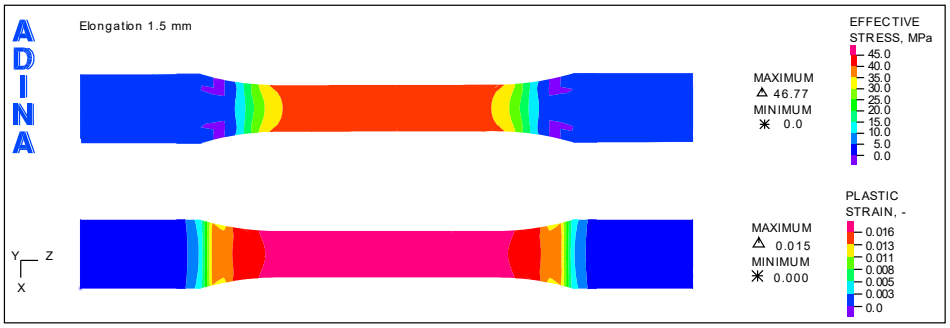

Fig. 7. Distributions of effective stresses and plastic strains on samples with geometry in accordance with ASTM D638

4. Discussion

A summary of the results of the modulus of elasticity, tensile strength and engineering strains at the moment of reaching the tensile strength for all 60 samples is shown in Figure 8.

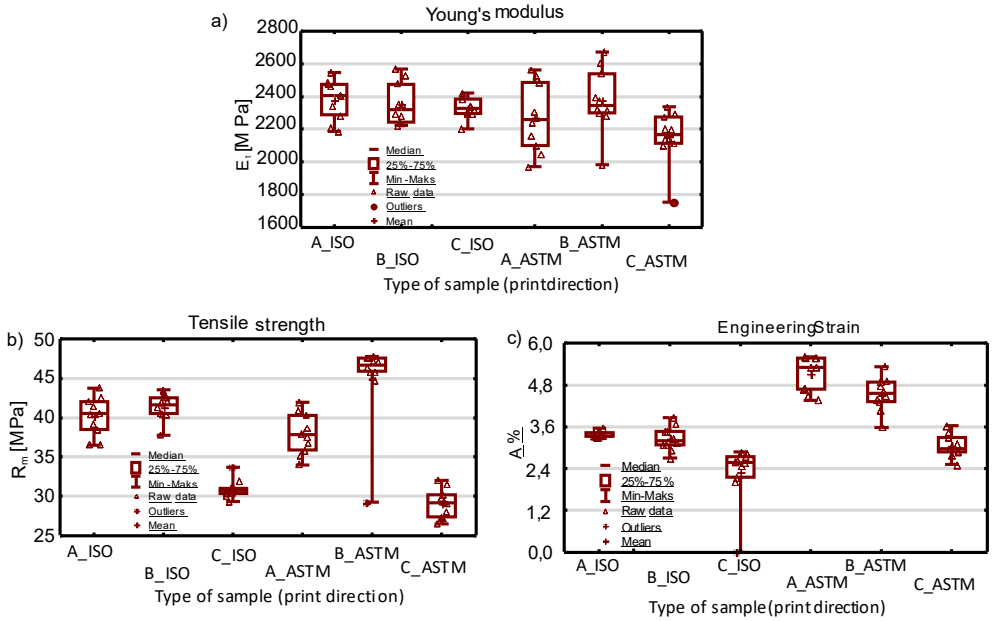

Fig. 8. Distributions of effective stresses and plastic strains on samples with geometry in accordance with ASTM D638

Analysing Figure 8a, it can be observed that the value of the modulus of elasticity does not depend on the direction of the printouts of samples or on the geometry of the samples. Considering the tensile strength (Fig. 8b), both the geometry of the samples and the direction of the print affect the strength values. The tensile strength is higher for samples in which the printing direction is parallel to the direction of stretching (type A and B). The lowest tensile strength is shown by samples whose stretching and print directions are perpendicular (type C).

Differences in results between samples made in accordance with the ISO and ASTM standards depend on the dimensions of the measured part of the sample and the number of bonds between the print paths.

5. Conclusions

- The modulus of elasticity of the printouts does not depend on the direction of the printouts or on the geometry of the samples.
- The tensile strength of the prints depends on the geometry of the samples. The tensile strength of ISO-3167 geometries is greater than ASTM D638 geometries (with the same print direction).
- The tensile strength depends on the direction of the prints. The highest strength is achieved by printouts in which the increase in height during the FFF process corresponds to the thickness of the printouts. The lowest strength is achieved by printouts in which the increase in height during FFF corresponds to the direction of loading.
- The engineering strain of the prints depends on the geometry and direction of the prints. The strain of prints with geometry according to the ISO-3167 standard is smaller than the printouts with geometry according to the ASTM D638 standard (with the same direction of printouts).

References

[1] Li T., Wang L., Bending behavior of sandwich composite structures with tunable 3D-printed core materials, Composite Structures 2017, 175, 46-57, DOI: 10.1016/j.compstruct.2017.05.001.

[2] Osman R.B., van der Veen A.J., Huiberts D., Wismeijer D., Alharbi N., 3D-printing zirconia implants; a dream or a reality? An in-vitro study evaluating the dimensional accuracy, surface topography and mechanical properties of printed zirconia implant and discs, Journal of the Mechanical Behavior of Biomedical Materials 2017, 75, 521-528, DOI: 10.1016/j.jmbbm.2017.08.018.

[3] Cano-Vicent A., Tambuwala M.M., Hassan S.S., Barh D., Aljabali A.A., Birkett M., Arjunan A., Serrano-Aroca Á., Fused deposition modelling: Current status, methodology, applications and future prospects, Additive Manufacturing 2021, 47, 102378, DOI: 10.1016/j.addma.2021.102378.

[4] DeStefano V., Khan S., Tabada A., Applications of PLA in modern medicine, Engineered Regeneration 2020, 1, 76-87, DOI: 10.1016/j.engreg.2020.08.002.

[5] Gonabadi H., Chen Y., Yadav A., Bull S., Investigation of the effect of raster angle, build orientation, and infill density on the elastic response of 3D printed parts using finite element microstructural modeling and homogenization techniques, Journal of Advanced Manufacturing Technology 2022, 118(5-6), 1485-1510, DOI: 10.1007/s00170-021-07940-4.

[6] International Standard (ISO), 2014, Plastics – Multipurpose test specimens (ISO-3167).

[7] D20 Committee, 2014, Standard Test Method for Tensile Properties of Plastics, ASTM International, West Conshohocken (ASTM D638-14). Accessed 3 March 2019.

Eksperymentalna i numeryczna ocena właściwości mechanicznych wydruków 3D wykonanych metodą druku przyrostowego

STRESZCZENIE:
Przedstawiono zarówno wyniki badań, jak i obliczenia numeryczne wydruków 3D wykonanych z wykorzystaniem metody druku przyrostowego (FFF) wykonanych z filamentu PLA. Celem pracy było określenie własności mechanicznych. Zaobserwowano, że moduł Younga wydruków nie zależy od geometrii próbek ani od kierunku wydruków, natomiast wytrzymałość na rozciąganie i odkształcenia wydruków zależą od geometrii oraz od kierunku wydruków w stosunku do kierunku obciążania.

SŁOWA KLUCZOWE:
druk 3D; FFF; statyczna próba rozciągania; MES